

## Structure-Function Studies of Artemisia tridentata Farnesyl Diphosphate Synthase and Chrysanthemyl Diphosphate Synthase by Site-Directed Mutagenesis and Morphogenesis

J. Scott Lee, Jian-Jung Pan, Gurusankar Ramamoorthy, and C Dale Poulter

*J. Am. Chem. Soc.*, **Just Accepted Manuscript** • DOI: 10.1021/jacs.7b07608 • Publication Date (Web): 19 Sep 2017

Downloaded from <http://pubs.acs.org> on September 19, 2017

### Just Accepted

“Just Accepted” manuscripts have been peer-reviewed and accepted for publication. They are posted online prior to technical editing, formatting for publication and author proofing. The American Chemical Society provides “Just Accepted” as a free service to the research community to expedite the dissemination of scientific material as soon as possible after acceptance. “Just Accepted” manuscripts appear in full in PDF format accompanied by an HTML abstract. “Just Accepted” manuscripts have been fully peer reviewed, but should not be considered the official version of record. They are accessible to all readers and citable by the Digital Object Identifier (DOI®). “Just Accepted” is an optional service offered to authors. Therefore, the “Just Accepted” Web site may not include all articles that will be published in the journal. After a manuscript is technically edited and formatted, it will be removed from the “Just Accepted” Web site and published as an ASAP article. Note that technical editing may introduce minor changes to the manuscript text and/or graphics which could affect content, and all legal disclaimers and ethical guidelines that apply to the journal pertain. ACS cannot be held responsible for errors or consequences arising from the use of information contained in these “Just Accepted” manuscripts.



1  
2  
3  
4  
5  
6  
7  
8  
9  
10  
11  
12  
13  
14  
15  
16  
17  
18  
19  
20  
21  
22  
23  
24  
25  
26  
27  
28  
29  
30  
31  
32  
33  
34  
35  
36  
37  
38  
39  
40  
41  
42  
43  
44  
45  
46  
47  
48  
49  
50  
51  
52  
53  
54  
55  
56  
57  
58  
59  
60

Structure-Function Studies of *Artemisia tridentata* Farnesyl  
Diphosphate Synthase and Chrysanthemyl Diphosphate  
Synthase by Site-Directed Mutagenesis and Morphogenesis

J. Scott Lee,<sup>†</sup> Jian-Jung Pan, Gurusankar Ramamoorthy and C. Dale  
Poulter\*

Department of Chemistry  
University of Utah  
315 South 1400 East, RM 2020  
Salt Lake City, UT 84112

1  
2  
3 **Abstract.** The amino acid sequences of farnesyl diphosphate synthase (FPPase) and  
4 chrysanthemyl diphosphate synthase (CPPase) from *Artemisia tridentata* ssp. *Spiciformis*,  
5 minus their chloroplast targeting regions, are 71% identical and 90% similar. FPPase  
6 efficiently and selectively synthesizes the “regular” sesquiterpenoid farnesyl diphosphate  
7 (FPP) by coupling isopentenyl diphosphate (IPP) to dimethylallyl diphosphate (DMAPP)  
8 and then to geranyl diphosphate (GPP). In contrast, CPPase is an inefficient promiscuous  
9 enzyme, which synthesizes the “irregular” monoterpenes chrysanthemyl diphosphate  
10 (CPP), lavandulyl diphosphate (LPP), and trace quantities of maconelliyl diphosphate  
11 (MPP) from two molecules of DMAPP, and couples IPP to DMAPP to give GPP. *A. tridentata*  
12 FPPase and CPPase belong to the chain elongation protein family (PF00348), a subgroup of  
13 the terpenoid synthase superfamily (CL0613) whose members have a characteristic  $\alpha$   
14 terpene synthase  $\alpha$ -helical fold. The active sites of *A. tridentata* FPPase and CPPase are  
15 located within a six-helix bundle containing amino acids 53 to 241. The two enzymes were  
16 metamorphosed into one another sequentially replacing the loops and helices of the six-  
17 helix bundle from enzyme with those from the other. Chain elongation was the dominant  
18 activity during the N-terminal to C-terminal metamorphosis of FPPase to CPPase, with  
19 product selectivity gradually switching from FPP to GPP, until replacement of the final  $\alpha$ -  
20 helix, whereupon cyclopropanation and branching activity competed with chain elongation.  
21 During the corresponding metamorphosis of CPPase to FPPase, cyclopropanation and  
22 branching activities were lost upon replacement of the first helix in the six-helix bundle.  
23 Mutations of active site residues in CPPase to the corresponding amino acids in FPPase  
24 enhanced chain-elongation activity, while similar mutations in the active site of FPPase  
25 failed to significantly promote formation of significant amounts of irregular monoterpenes.  
26  
27  
28  
29  
30  
31  
32  
33  
34  
35  
36  
37  
38  
39  
40  
41  
42  
43  
44  
45  
46  
47  
48  
49  
50  
51  
52  
53  
54  
55  
56  
57  
58  
59  
60

1  
2  
3 Our results indicate that CPPase, a promiscuous enzyme, is more plastic toward acquiring  
4 new activities; whereas, FPPase is more resistant. Mutations of residues outside of the  $\alpha$   
5  
6  
7  
8  
9  
10  
11  
12  
13  
14  
15  
16  
17  
18  
19  
20  
21  
22  
23  
24  
25  
26  
27  
28  
29  
30  
31  
32  
33  
34  
35  
36  
37  
38  
39  
40  
41  
42  
43  
44  
45  
46  
47  
48  
49  
50  
51  
52  
53  
54  
55  
56  
57  
58  
59  
60

LPP, and MPP.

## INTRODUCTION

1  
2  
3  
4  
5  
6  
7  
8  
9  
10  
11  
12  
13  
14  
15  
16  
17  
18  
19  
20  
21  
22  
23  
24  
25  
26  
27  
28  
29  
30  
31  
32  
33  
34  
35  
36  
37  
38  
39  
40  
41  
42  
43  
44  
45  
46  
47  
48  
49  
50  
51  
52  
53  
54  
55  
56  
57  
58  
59  
60

Isoprenoid compounds are readily distinguished from other natural products by the distinctive methylbutyl (isoprene) units embedded within their carbon skeletons. With over 80,000 members,<sup>1</sup> they constitute the largest and most structurally diverse group of compounds synthesized in nature.<sup>1</sup> Common metabolites of the isoprenoid biosynthetic pathway include sterols, carotenoids, ubiquinones, and mono-, sesqui-, and diterpenes.<sup>1-3</sup> The carbon skeletons of isoprenoid compounds are constructed from the fundamental C<sub>5</sub> isomeric building blocks isopentenyl diphosphate (IPP) and dimethylallyl diphosphate (DMAPP), which are joined by chain elongation (1'-4), branching (1'-2), cyclopropanation (c1'-2-3), and cyclobutanation (c1'-2-3-2') reactions (Figure 1).<sup>2</sup> The 1'-4 pattern is the most common attachment found between isoprene units and is typically called a "regular" or "head-to-tail" coupling.<sup>4</sup> The other three are termed "irregular" or "non-head-to-tail".<sup>5</sup> The 1'-4 pattern results from a reaction that joins C1 in DMAPP, or its higher isoprenologs, to C4 in IPP. Thus, beginning with DMAPP, a homologous series of linear C<sub>10</sub>, C<sub>15</sub>, C<sub>20</sub>, etc. allylic diphosphates is formed, where each member can be the substrate for construction of more complex skeletons, including those with c1'-2-3, 1'-2, and c1'-2-3-2' substructures.<sup>2</sup>

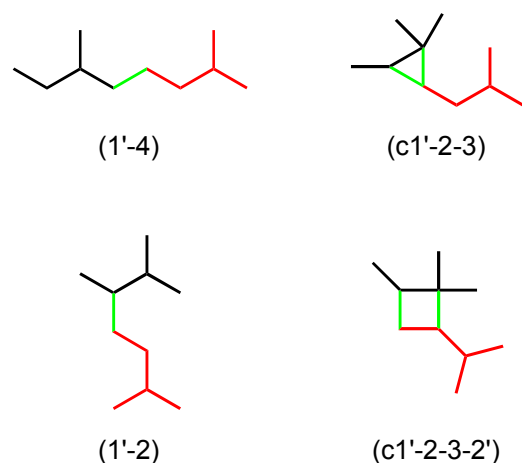


**Figure 1.** Four basic patterns for incorporation of isoprene units into metabolites by joining two isoprenoid diphosphates. Bonds between isoprene units are in green. The isoprene units are numbered according to the numbering schemes for IPP and DMAPP.

Two structurally distinct families of enzymes catalyze chain elongation. While each contains enzymes selective for the synthesis of products with different chain lengths, one family synthesizes allylic isoprenoid diphosphates with *E*-double bonds, and the other, allylic diphosphates with *Z*-double bonds. *E*-polyprenyl diphosphate synthases typically produce short-chain products early in the isoprenoid pathway.<sup>6</sup> These enzymes belong to the chain elongation family (PF00348) within the terpenoid synthase superfamily (CL0613),<sup>7</sup> whose members also include protein families for cyclopropanation/rearrangement (PF00494) and cyclization (PF03936 and PF01397) (Figure 2). While all proteins in CL0613 contain a characteristic all  $\alpha$ -helix  $\alpha$  terpene synthase motif,<sup>7-9</sup> those belonging to PF03936 and PF01397 often have additional  $\beta$  and/or  $\gamma$  domains.<sup>10</sup> Enzymes in the *Z*-polyprenyl synthase family belong to PF01255 and synthesize longer-chain products.<sup>11,12</sup>

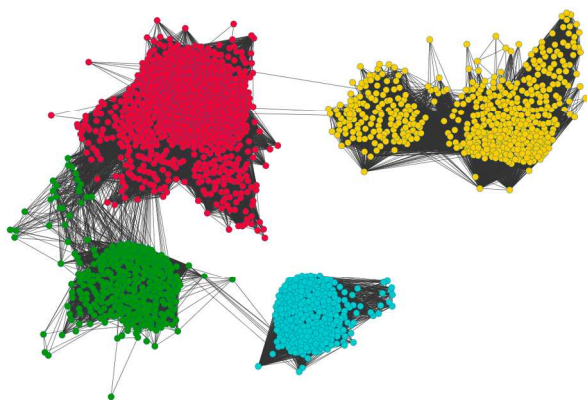
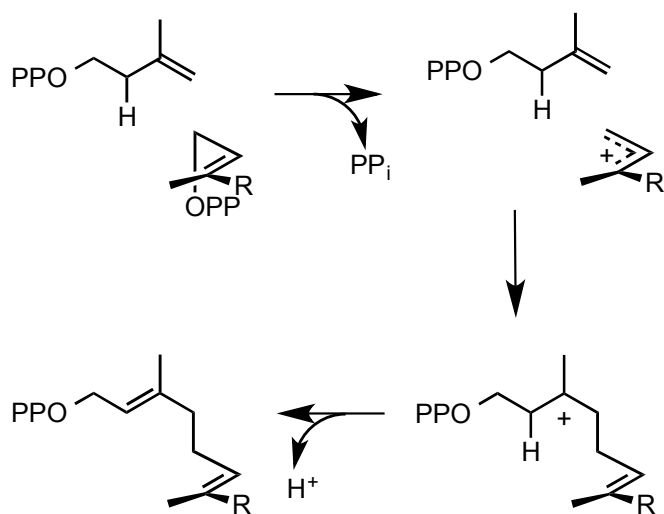


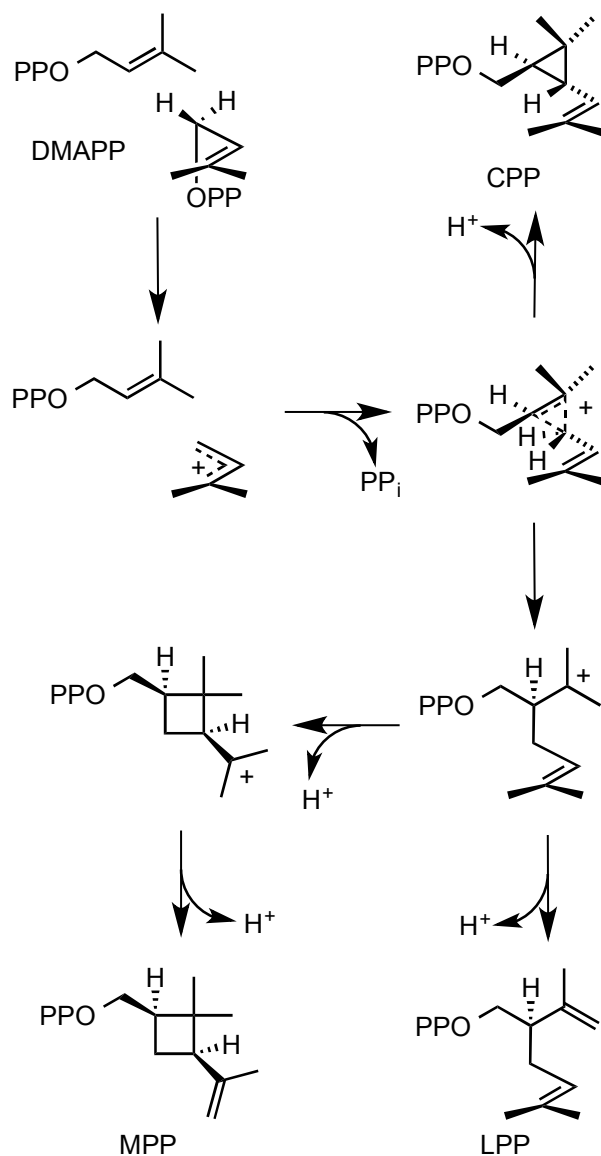
**Figure 2.** Sequence similarity network (Blast cut-off of  $e^{-7}$ ) for enzymes in the terpenoid synthase superfamily (CL0613); chain elongation (PF00348, red), cyclopropanation/rearrangement (PF00494, gold), cyclization (PF03936, green; PF01397, turquoise).

Chain elongation is the most common reaction in the isoprenoid pathway. The first step in *E*-selective chain elongation couples DMAPP and IPP to produce geranyl diphosphate (GPP). GPP can then couple with another molecule of IPP to give farnesyl diphosphate (FPP), and so on.<sup>4</sup> The isoprene units are joined by a dissociative electrophilic alkylation of the nucleophilic double bond in IPP by an electrophilic cation generated from the allylic diphosphate cosubstrate (DMAPP, GPP, FPP, etc.) (Scheme 1).<sup>13, 14</sup> Extension of the allylic chain by sequential addition of molecules of IPP produces a homologous series of allylic isoprenoid diphosphates that in turn are substrates for branch point enzymes that feed into the numerous branches of the terpenoid pathway.<sup>15</sup>



**Scheme 1.** Electrophilic alkylation mechanism for chain elongation. R = CH<sub>3</sub>, C<sub>6</sub>H<sub>11</sub>, C<sub>11</sub>H<sub>19</sub>, etc.

The cyclopropanation reaction is also common, but this linkage is subsequently disassembled in most metabolites and is typically detected indirectly through rearranged carbon skeletons in downstream metabolites.<sup>16</sup> For example, the first pathway specific carbon skeletons in downstream metabolites.<sup>16</sup> For example, the first pathway specific reaction in biosynthesis of sterols and carotenoids is a c1'-2-3 cyclopropanation, followed by a rearrangement to give structures with 1'-1 (head-to-head) linkages between the two component isoprenoid fragments.<sup>17, 18</sup> The mechanism for cyclopropanation is also a dissociative electrophilic alkylation, where the allylic cation generated by one molecule of an allylic diphosphate attacks the allylic double bond in another molecule, as illustrated for the coupling of DMAPP to give chrysanthemyl diphosphate (CPP) in Scheme 2.<sup>2</sup> Metabolites with structures derived from 1'-2 branching, as illustrated by lavandulyl diphosphate (LPP), are much less common,<sup>19</sup> while those with 1'-2-3-2' cyclobutane structures, illustrated by maconelliyl diphosphate (MPP), have only been reported for mealy bug mating pheromones.<sup>20,21</sup> The 1'-2 and c1'-2-3-2' structures are produced from the same protonated cyclopropane intermediates that give the c1'-2-3 skeletons.<sup>2,22</sup>



**Scheme 2.** An integrated electrophilic alkylation-rearrangement mechanism for formation of cyclopropane, branched, and cyclobutane skeletons.

Enzymes that catalyze c1'-2-3 cyclopropanation typically couple two molecules of DMAPP to give chrysanthemyl diphosphate (CPP),<sup>22</sup> two molecules of FPP to give presqualene diphosphate,<sup>23,24</sup> or two molecules of geranylgeranyl diphosphate to give prephytoene diphosphate.<sup>25</sup> Presqualene and prephytoene diphosphates are intermediates in the sterol and carotenoid pathways, respectively. Enzymes that catalyze 1'-2 branching

1  
2  
3 are found in PF00348 and the structurally unrelated Z-polyprenyl synthase family  
4  
5 PF01255.<sup>26</sup> The only wild-type enzyme known to catalyze c1'-2-3-2' cyclobutanation is  
6  
7  
8 CPPase, where cyclobutanation is a minor promiscuous activity.  
9

10 The enzymes in CL0613 have distinctive aspartate/glutamate-rich sequences that,  
11  
12 along with Mg<sup>2+</sup> ions, bind the diphosphate moieties of their substrates and catalyze  
13  
14 carbocation formation.<sup>27,28</sup> The structures of proteins in PF00348 and PF00494 suggest  
15  
16 that they diverged from a common chain elongation ancestor early in the evolution of  
17  
18 terpenoid biosynthesis.<sup>10</sup> This hypothesis is supported by the recent emergence of a new  
19  
20 cyclopropanation enzyme, chrysanthemyl diphosphate synthase (CPPase) in  
21  
22 chrysanthemums (*Chrysanthemum cinerariifolium*)<sup>22</sup> and sagebrush (*Artemisia tridentata*  
23  
24 ssp. *Spiciformis*)<sup>29</sup> from farnesyl diphosphate synthase (FPPase) in the same plants. The  
25  
26 chain elongation and cyclopropanation enzymes are members of PF00348 and share  
27  
28 structural features found in other chain elongation enzymes in that family.<sup>6</sup> *A. tridentata*  
29  
30 contains two FPPases that are highly selective and efficient for chain elongation of DMAPP  
31  
32 to FPP. In contrast, *A. tridentata* CPPase is an inefficient, promiscuous enzyme that  
33  
34 converts two molecules of DMAPP to CPP (c1'-2-3, cyclopropanation), lavandulyl  
35  
36 diphosphate (LPP, 1'-2, branching), and maconelliyl diphosphate (MPP, c1'-2-3-2',  
37  
38 cyclobutanation), as well as IPP and DMAPP to GPP (1'-4, chain elongation). These  
39  
40 properties are consistent with those expected for recently evolved enzyme that has gained  
41  
42 a new function but has not yet optimized its ability to catalyze the new reaction.<sup>30</sup>  
43  
44  
45  
46  
47  
48  
49  
50

51 *E*-Polyprenyl chain elongases have five conserved regions within a six-helix bundle  
52  
53 that contains characteristic aspartate-rich DDxx(xx)D diphosphate binding motifs.<sup>31,32</sup>  
54  
55 Differences between *A. tridentata* FPPase and CPPase within this bundle are minimal. The  
56  
57  
58  
59  
60

1  
2  
3 substantial similarity between FPPase and CPPase prompted us to construct chimeric *A.*  
4 *tridentata* proteins where FPPase was transformed into CPPase, and vice versa, by  
5 replacing conserved regions of one enzyme with those from the other.<sup>6</sup> The constructs  
6 retained the ability to catalyze chain elongation while acquiring the ability to catalyze  
7 branching, cyclobutanation and cyclopropanation. We now present product and kinetic  
8 studies for chimeras where each helix and loop between the first and last helix in the six-  
9 helix bundle in one enzyme is replaced by the corresponding sequence in the other and for  
10 site-directed mutants where only active-site residues are replaced. Our results illustrate  
11 the importance of residues outside of the active site to influence the regioselectivity of the  
12 reactions.  
13  
14  
15  
16  
17  
18  
19  
20  
21  
22  
23  
24  
25  
26  
27  
28  
29

## 30 RESULTS

31  
32 *Engineered proteins. i. Chimeras.* Chimeric enzymes were constructed from *A.*  
33 *tridentata* FPPase and CPPase by replacing the amino acids in one protein with those from  
34 the other at 13 different junctions, beginning at the N-terminus using megaprimer whole  
35 plasmid (MEGAWHOP) and structure-based combinatorial protein engineering (SCOPE)  
36 PCR protocols.<sup>33,34</sup> The first PCR reaction synthesized a megaprimer that codes for amino  
37 acid sequences from the N-terminus of the chimeric proteins, fused at the appropriate  
38 junction site, to a short segment that codes for amino acids in the C-terminal segment. The  
39 second PCR synthesized an expression plasmid for the chimeric protein (Figure S1).  
40  
41  
42  
43  
44  
45  
46  
47  
48  
49  
50

51 Names for the chimeras are based on the enzyme from which the N-terminal  
52 sequence was derived, F for FPPase or C for CPPase, and the junction at which the sequence  
53 changes to the other enzyme. For instance, the “C6” chimera consists of CPPase sequence  
54  
55  
56  
57  
58  
59  
60

1  
2  
3 from the N-terminus to the sixth junction, with the remaining sequence from FPPase (see  
4 Figure 3). The precise locations of the helices were identified by comparisons of X-ray  
5 structures for FPPase and confirmed by the structure of chimera C3. Chimeras were  
6 constructed from FPPase and CPPase by fusing the proteins at 13 junctions to produce  
7 chimeric fusions at each helix/loop transition from amino acids 53 to 241, including the  
8 junction between amino acids 193 and 194 located on either side of a kink in helix VII. Two  
9 additional FPPase-CPPase chimeras constructed where the six-helix bundle consisting of  
10 sequences from amino acids 53 to 241 from one enzyme (core) were flanked with the  
11 corresponding N- and C-terminal sequences (scaffold) from the other. These core-scaffold  
12 chimeras, with cores from FPPase and CPPase, are named c-F-c and f-C-f, respectively.  
13  
14  
15  
16  
17  
18  
19  
20  
21  
22  
23  
24  
25  
26  
27  
28  
29  
30  
31  
32  
33  
34  
35  
36  
37  
38  
39  
40  
41  
42  
43  
44  
45  
46  
47  
48  
49  
50  
51  
52  
53  
54  
55  
56  
57  
58  
59  
60

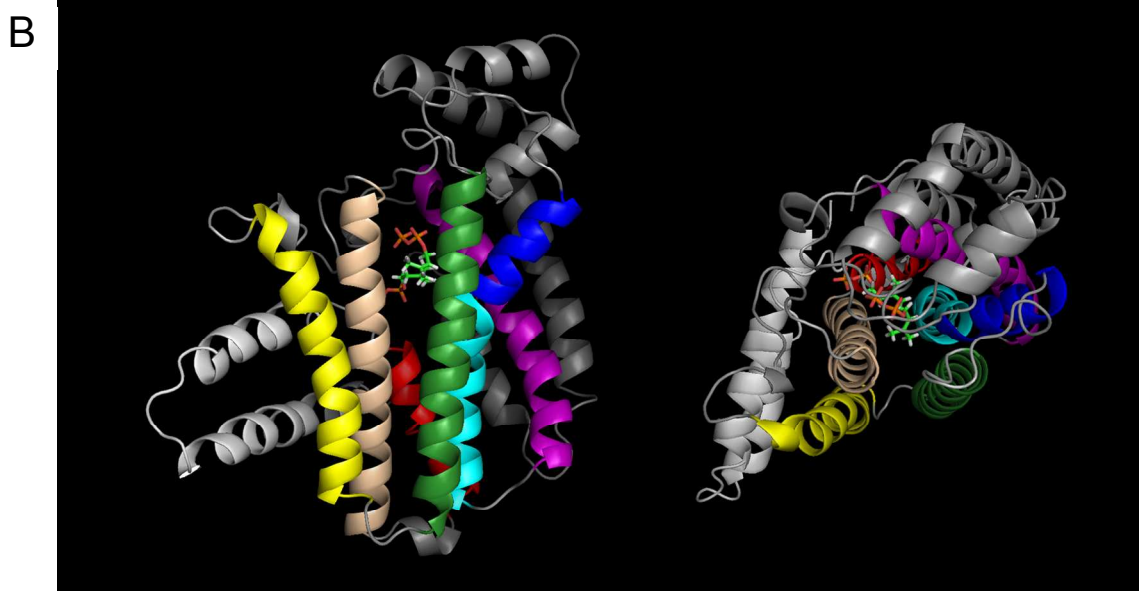
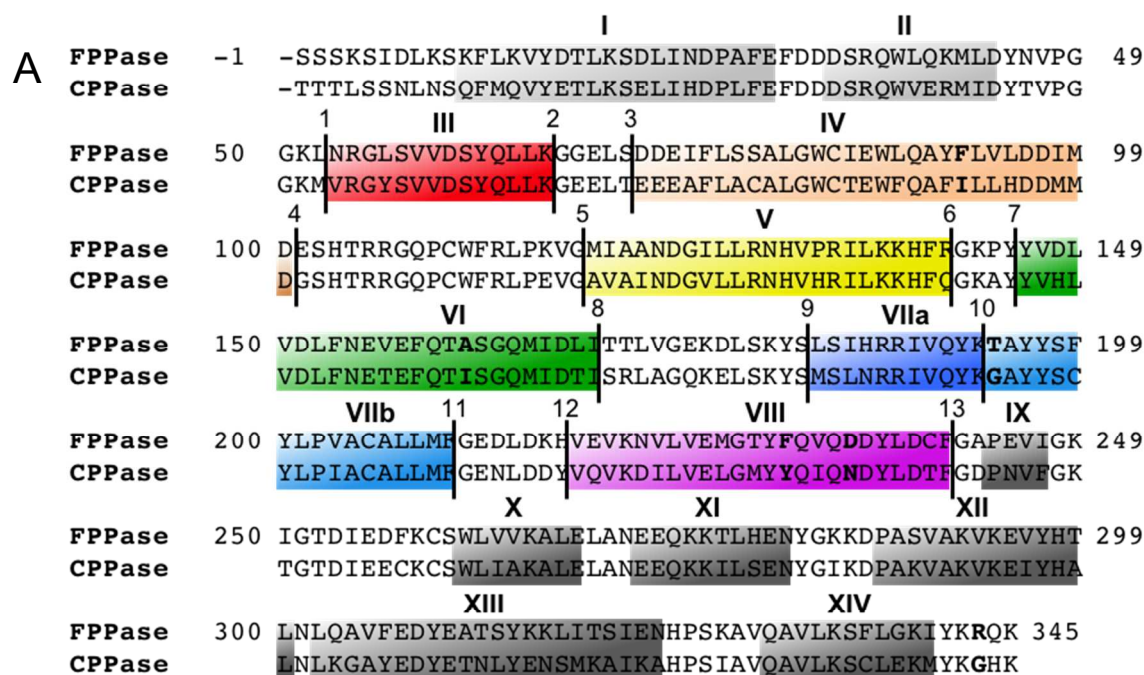


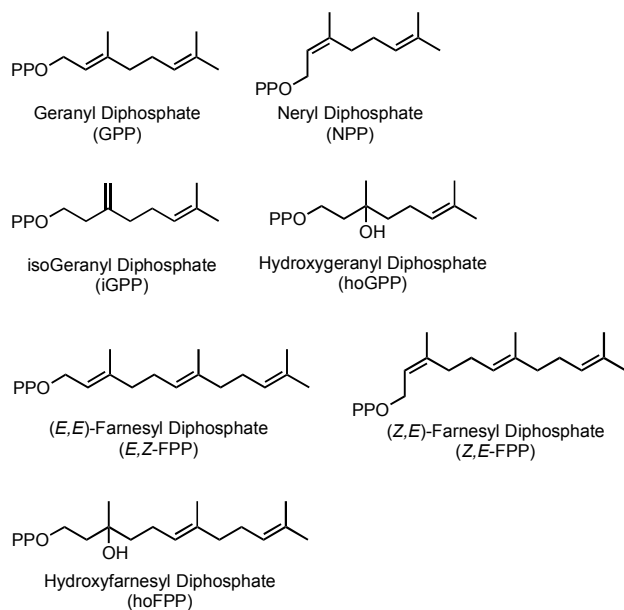
**Figure 3.** Part A. Sequence alignments for *A. tridentata* FPPase and CPPase, where helices in the N-terminal sequence (light gray), six-helix bundle (colored), and C-terminal regions are highlighted. K193 and T194 lie on either side of a kink between helix VIIa (dark blue) and helix VIIb (cyan). The thirteen junctions used for morphogenesis are located at the beginning and end of each helix and at the KT junction at the kink between VIIa and VIIb. Active site residues in CPPase that are different from those of FPPase are in bold. Part B. Ribbon structures from the side and the top of a subunit in the *A. tridentata* FPPase homodimer.

1  
2  
3  
4  
5  
6 ii. Site-Directed Mutants. Six amino acids in the active site of FPPase (F92, A161,  
7  
8 T194, F231, D235 and R343) differ from the corresponding residues in CPPase (I92, I161,  
9  
10 G194, Y231, N235, and G343). In FPPase, F92 and A161 form part of the binding pocket for  
11  
12 the hydrocarbon moieties in DMAPP and GPP, the polar amino acids are in contact with the  
13  
14 diphosphate residues or the tightly bound  $Mg^{2+}$  ions, and F231 and D235 form part of the  
15  
16 binding pocket for the hydrocarbon moiety in IPP. Substitution of A161 by I161 shortens  
17  
18 the binding pocket for the hydrocarbon moiety of the allylic substrate in CPPase,  
19  
20 decreasing the preference for binding GPP over DMAPP. Ten site-directed mutants of  
21  
22 FPPase and CPPase were constructed where one, or a combination of, the active site  
23  
24 residues in one enzyme were replaced with those from the other to give FPPase single  
25  
26 mutants A161I, T194G, F231Y, D235N, double mutant F231Y/D235N (2mFPPase), triple  
27  
28 mutant A161I/T194G/D235N (3mFPPase), quintuple mutant A161I/T194G/  
29  
30 F231Y/D235N/ R343G (5mFPPase) and sextuple mutant  
31  
32 F92I/A161I/T194G/F231Y/D235N/R343G (6mFPPase); and CPPase single mutant N235D  
33  
34 and triple-mutant I161A/G194T/N235D (3mCPPase). All of the mutants contained an N-  
35  
36 terminal His<sub>6</sub> tag to facilitate purification by Ni<sup>2+</sup> affinity chromatography.  
37  
38  
39  
40  
41  
42  
43

44 *Product studies.* Products were determined for incubations with 0.5 mM IPP and 0.5  
45  
46 mM DMAPP (chain elongation conditions), which gave products from chain elongation,  
47  
48 cyclopropanation, branching, and cyclobutanation reactions, and with 3 mM DMAPP  
49  
50 (irregular conditions), which only gave products from cyclopropanation, branching, and  
51  
52 cyclobutanation reactions. The structures and relative amounts of products were  
53  
54 determined by hydrolysis of the diphosphates with alkaline phosphatase, extraction of the  
55  
56  
57  
58  
59  
60

corresponding alcohols with methyl *tert*-butyl ether (MTBE), and analysis by GC on HP-5 or Chiral-HP GC columns and by GC/MS. Structures were established by comparing GC retention times and mass spectra with authentic samples (Figure 4).<sup>6</sup>

#### Chain Elongation



#### Cyclopropanation, Branching, Cyclobutanation

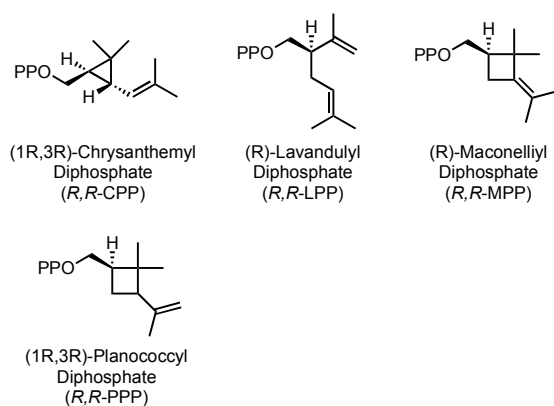


**Figure 4.** Products from FPPase, CPPase, and FPPase/CPPase chimeras and site-directed mutants.

Under standard chain elongation conditions, FPPase gave *E,E*-FPP as the major product, accompanied by a smaller amounts of GPP and the *Z,E*-FPP (Table 1).<sup>14</sup> Since formation of FPP requires two molecules of IPP and equal concentrations of IPP and DMAPP were used in the incubations, at the point where IPP was exhausted, only ~55% of the available DMAPP had been consumed to give an 11:1 ratio of *E,E*-FPP: GPP. The preponderance of *E,E*-FPP reflects substantial preference for utilization of GPP over DMAPP for chain elongation.<sup>35</sup>

**Table 1.** Relative percentages of products formed by FPPase, CPPase, chimeras and site-directed mutants under chain elongation incubation conditions (0.5 mM DMAPP and IPP) (GPP, geranyl diphosphate; NPP, neryl diphosphate; iGPP, isogeranyl diphosphate; hoGPP, hydroxygeranyl diphosphate; *E,E*-FPP, *E,E*-farnesyl diphosphate; *Z,E*-FPP, *Z,E*-farnesyl diphosphate; hoFPP, hydroxyfarnesyl diphosphate; CPP, chrysanthemyl diphosphate; LPP, lavandulyl diphosphate).

	GPP	NPP	iGPP	hoGPP	<i>E,E</i> -FPP	<i>Z,E</i> -FPP	hoFPP	CPP	LPP
<b>FPPase</b>	8 ± 1	<1	nd	nd	88 ± 1	4 ± 1	nd	nd	nd
C1	9 ± 2	<1	nd	nd	87 ± 2	4 ± 1	nd	nd	nd
C2	21 ± 1	<1	nd	nd	76 ± 1	3 ± 1	nd	nd	nd
C3	7 ± 1	<1	nd	nd	90 ± 1	2 ± 1	nd	nd	nd
C4	16 ± 1	<1	nd	nd	81 ± 1	3 ± 1	nd	nd	nd
C5	22 ± 3	1 ± 1	nd	nd	75 ± 3	2 ± 1	nd	nd	nd
C6	51 ± 6	2 ± 1	nd	nd	47 ± 6	<1	nd	nd	nd
C7	60 ± 2	2 ± 1	nd	nd	38 ± 2	<1	nd	nd	nd
C8	66 ± 2	2 ± 1	nd	nd	31 ± 2	nd	nd	nd	nd
C9	92 ± 1	3 ± 1	nd	nd	3 ± 2	nd	nd	nd	nd
C10	76 ± 2	2 ± 1	nd	nd	21 ± 2	nd	nd	nd	nd
C11	70 ± 4	2 ± 1	nd	nd	27 ± 4	nd	nd	nd	nd
C12	85 ± 1	3 ± 1	nd	nd	10 ± 1	nd	nd	nd	nd
C13	63 ± 1	2 ± 1	nd	nd	22 ± 1	nd	nd	3 ± 1	8 ± 1
A161I	21 ± 2	2 ± 1	nd	nd	70 ± 2	7 ± 1	nd	nd	nd
T194G	7 ± 1	<1	nd	nd	85 ± 2	8 ± 1	nd	nd	nd
F231Y	71 ± 2	<1	nd	nd	29 ± 1	<1	nd	nd	nd
D235N	9 ± 1	<1	nd	nd	84 ± 2	7 ± 1	nd	nd	nd

2m	71 ± 2	nd	nd	nd	29 ± 1	nd	nd	nd	nd
3m	62 ± 3	nd	nd	nd	29 ± 1	9 ± 1	nd	nd	nd
5m	69 ± 3	5 ± 1	nd	nd	24 ± 1	2 ± 1	nd	nd	nd
6m	93 ± 3	3 ± 1	nd	nd	4 ± 3	<1	nd	nd	nd
c-F-c	12 ± 3	nd	nd	nd	88 ± 3	nd	nd	nd	nd
<b>CPPase</b>	47 ± 1	3 ± 1	2 ± 1	nd	2 ± 1	nd	nd	35 ± 1	11 ± 1
F1	65 ± 1	2 ± 1	<1	nd	4 ± 1	nd	nd	18 ± 1	11 ± 1
F2	93 ± 1	2 ± 1	<1	nd	4 ± 1	nd	nd	nd	nd
F3	81 ± 6	2 ± 1	<1	nd	19 ± 6	<1	nd	nd	nd
F4	76 ± 2	2 ± 1	<1	nd	24 ± 2	<1	nd	nd	nd
F5	65 ± 2	1 ± 1	nd	nd	33 ± 2	1 ± 1	nd	nd	nd
F6	72 ± 3	1 ± 1	nd	nd	28 ± 3	<1	nd	nd	nd
F7	55 ± 6	1 ± 1	nd	nd	43 ± 4	1 ± 1	nd	nd	nd
F8	14 ± 2	<1	nd	nd	81 ± 2	3 ± 1	nd	nd	nd
F9	8 ± 2	nd	nd	nd	89 ± 2	3 ± 1	nd	nd	nd
F10	26 ± 1	<1	nd	nd	72 ± 1	2 ± 1	nd	nd	nd
F11	38 ± 4	<1	nd	nd	60 ± 4	2 ± 1	nd	nd	nd
F12	53 ± 4	1 ± 1	nd	nd	46 ± 4	<1	nd	nd	nd
F13	21 ± 5	<1	nd	nd	76 ± 5	3 ± 1	nd	nd	nd
N235D	63 ± 3	4 ± 1	7 ± 1	22 ± 1	nd	nd	nd	<1	4 ± 1
3m	70 ± 2	5 ± 1	6 ± 1	17 ± 1	2 ± 1	<1	<1	nd	nd
f-C-f	68 ± 2	2 ± 1	nd	nd	nd	nd	nd	1 ± 0.3	25 ± 1

nd, not detected.

As the N- to C-terminal metamorphosis of FPPase into CPPase proceeded, FPP was the major product until the C6 chimera, where helix V was replaced and ~equal amounts of GPP and FPP were formed (Figure 5A). Small to trace amounts of NPP and *Z,E*-FPP were observed for the chimeras that produced substantial amounts of GPP and FPP, respectively. From the C6 chimera on, the amount of GPP was similar to or greater than FPP, reaching a maximum of 92% for C9. No irregular products were observed under chain elongation conditions until the metamorphosis had proceeded to C13, where all helices forming the active site bundle in FPPase had been replaced, at which point CPP and LPP constituted

~11% (~1:3 CPP:LPP) of the product mixture. Upon completion of the metamorphosis to CPPase, approximately equal amounts of chain elongation (mostly GPP) and irregular (~3:1 CPP:LPP) products were seen.

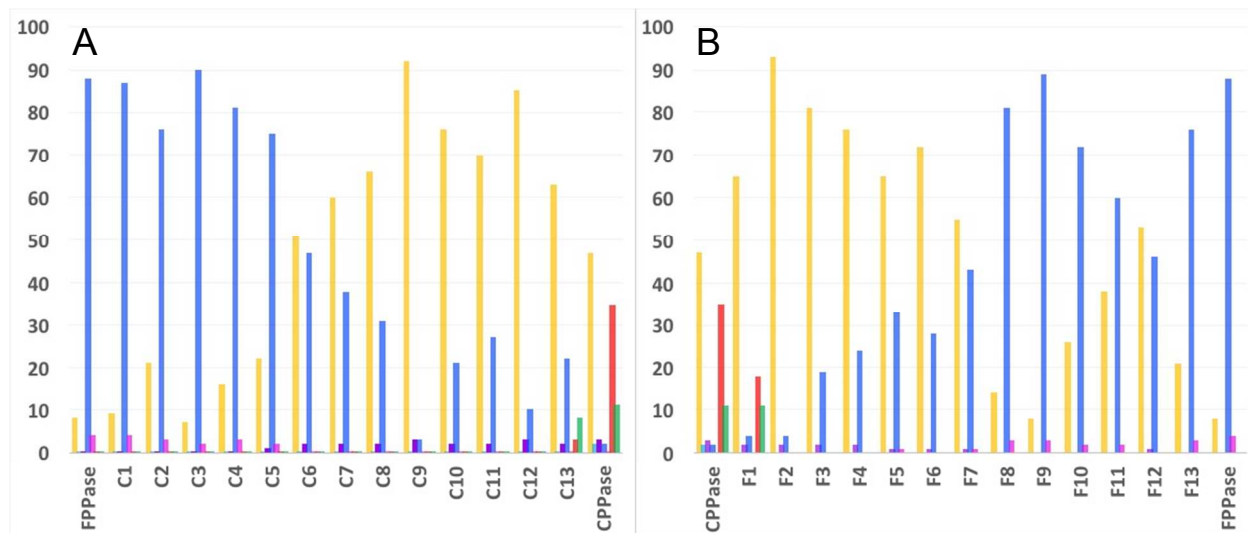


Figure 5. Products formed under chain elongation conditions during morphogenesis of FPPase to CPPase and of CPPase to FPPase. GPP, gold; *i*GPP, light blue; NPP, purple; *E,E*-FPP, dark blue; *Z,E*-FPP, pink; CPP, red; LPP, green. Part A, FPPase to CPPase; Part B, CPPase to FPPase.

The loss of activity for synthesis of irregular products was dramatic during the metamorphosis of CPPase to FPPase. Production of CPP and LPP plummeted upon replacement of helix III in F2 to give an enzyme that predominantly formed GPP. The remaining metamorphoses produced enzymes that mostly gave increasing amounts of FPP. Production of FPP increased steadily between F2 and F9, where it reached 90%, and decreased to 46% at F12 before rising again (Figure 5B).

The influence of the scaffolds surrounding the active-site helical bundles in FPPase and CPPase was evaluated with core-scaffold chimeras c-F-c and f-C-f. Synthesis of FPP

1  
2  
3 was predominant for F13, C1, and the core-scaffold c-F-c chimera. In contrast, more diverse  
4  
5 distributions were seen for C13, F1, and f-C-f. FPP, which constituted 23% of the product  
6  
7 mixture for C13, was detected at 4% for F1 and not detected for the f-C-f chimera.  
8  
9

10 Furthermore, the CPP:LPP ratios were ~1:3 for C13, ~2:1 for F1, and ~1:25 for f-C-f.

11  
12 These core-scaffold chimeras highlight the ability of amino acid substitutions outside of the  
13  
14 active site and even outside the  $\alpha$  terpenoid fold, to alter product distributions for the  
15  
16 promiscuous CPPase while minimally effecting those of the more robust FPPase.  
17  
18  
19

20  
21 Single replacements of active site residues in FPPase with the corresponding amino  
22  
23 acids in CPPase did not substantially alter the product distributions, with the exception of  
24  
25 the F231Y mutation, which almost reversed the relative amounts of GPP and FPP. None of  
26  
27 the FPPase mutants with multiple active site replacements gave irregular products in  
28  
29 incubations with IPP and DMAPP. In sharp contrast, a single N235D mutation in CPPase  
30  
31 substantially reduced the production of irregular products by reducing synthesis of CPP  
32  
33 and FPP, and instead gave GPP as the major product, along with 30% of a 1:3 mixture of  
34  
35 iGPP and hoGPP. Similar distributions of C<sub>10</sub> products were seen for 3mCPPase, along with  
36  
37 small amounts of both double bond isomers of FPP and hoFPP.  
38  
39  
40  
41

42  
43 Only products with irregular carbon skeletons were formed when the enzymes were  
44  
45 incubated with 3 mM DMAPP (irregular conditions). No products were seen for FPPase, C2,  
46  
47 C9, F2-F7, F11-F13, and c-F-c. LPP (branching) and MPP (cyclobutanation) were the only  
48  
49 products detected for chimeras C1, C3, C4, C8, C10, C11, and F10, as well as 5mFPPase and  
50  
51 6mFPPase (Table 2). The C5-C7 chimeras also produced trace amounts of planococcyll  
52  
53 diphosphate (PPP), a double bond isomer of MPP. CPP was first observed as a minor  
54  
55 product for C12 during the metamorphosis of FPPase to CPPase, and only became  
56  
57  
58  
59  
60

dominant for CPPase. C12, C13, F1, F8, F9, f-C-f, CPPase, the N235D CPPase mutant, and 3mCPPase synthesized compounds with all three of the irregular carbon skeletons.

**Table 2.** Relative percentages of products formed by the irregular coupling of two molecules of DMAPP.

	CPP	LPP	MPP	PPP
<b>FPPase</b>	nd	nd	nd	nd
C1	nd	66 ± 8	34 ± 8	nd
C3	nd	63 ± 5	37 ± 5	nd
C4	nd	48 ± 1	52 ± 1	nd
C5	nd	47 ± 2	50 ± 1	3 ± 1
C6	nd	58 ± 1	39 ± 1	3 ± 1
C7	nd	57 ± 2	40 ± 2	3 ± 1
C8	nd	56 ± 4	44 ± 4	nd
C10	nd	57 ± 1	43 ± 1	nd
C11	nd	94 ± 1	6 ± 1	nd
C12	2 ± 0.3	95 ± 1	3 ± 1	nd
C13	27 ± 0.5	72 ± 1	1 ± 1	nd
5m	nd	63 ± 2	37 ± 2	nd
6m	nd	89 ± 2	11 ± 1	nd
<b>CPPase</b>	79 ± 1	20 ± 1	1 ± 1	nd
F1	64 ± 1	35 ± 1	1 ± 1	nd
F8	5 ± 1	86 ± 1	9 ± 1	nd
F9	4 ± 1	86 ± 1	10 ± 1	nd
F10	nd	83 ± 1	17 ± 1	nd
N235D	19 ± 1	79 ± 1	2 ± 1	nd
3m	2 ± 1	80 ± 1	17 ± 1	nd
f-C-f	16 ± 0.7	83 ± 1	1 ± 1	nd

nd, not detected.

*Kinetic studies.* Apparent Michaelis-Menten constants were determined from single-point measurements of initial rates for product formation. [ $\beta$ - $^{32}$ P]IPP and [ $\beta$ - $^{32}$ P]DMAPP

1  
2  
3 were synthesized from the corresponding monophosphate esters by incubation with [ $\gamma$ -  
4  $^{32}\text{P}$ ]ATP and isopentenyl phosphate kinase.<sup>36</sup> After quenching, assay mixtures were spotted  
5  
6 on silica TLC plates and the developed plates analyzed by phosphorimaging. Radioactivity  
7  
8 only appeared in products from chain elongation for incubations with [ $\beta$ - $^{32}\text{P}$ ]IPP and  
9  
10 DMAPP. For chain elongation, values for  $k_{\text{cat}}$  and  $K_{\text{M}}$  were obtained by fits to the equations  
11  
12 for a sequential bisubstrate binding mechanism.<sup>37</sup> The equations for the coupling of two  
13  
14 molecule of DMAPP have squared terms for the substrate in the numerator and  
15  
16 denominator as the result of DMAPP binding at both the donor and acceptor sites.  
17  
18 Consequently, we could not obtain Michaelis constants for DMAPP binding at individual  
19  
20 donor and acceptor sites by varying [DMAPP] and instead report  $K_{50}^{\text{DMAPP}}$ , the  
21  
22 concentration of DMAPP that gives half-maximal velocity.  
23  
24  
25  
26  
27  
28  
29

30 The kinetic constants for chain elongation are presented in Table 3. We were not  
31  
32 able to measure values for chimeras C9 and F2-F7 because of a combination of low  
33  
34 activities and poor levels of expression. The catalytic efficiency for chain elongation of GPP  
35  
36 to FPP ( $\text{CE}^{\text{GPP}}$ , defined by  $k_{\text{cat}}^{\text{GPP}}/K_{\text{M}}^{\text{GPP}} = 2.4 \times 10^6 \text{ s}^{-1}\text{M}^{-1}$ ) by sagebrush FPPase was similar  
37  
38 to  $\text{CE}^{\text{GPP}}$  for the avian enzyme and approximately 100-fold slower than the diffusion  
39  
40 controlled limit for substrate binding (Table 4).<sup>35</sup>  $\text{CE}^{\text{DMAPP}}$  for chain elongation of DMAPP to  
41  
42 GPP was ~20-fold lower. This difference favors synthesis of FPP and minimizes  
43  
44 accumulation of GPP during chain elongation from DMAPP to FPP. The values for  $\text{CE}^{\text{DMAPP}}$   
45  
46 and  $\text{CE}^{\text{GPP}}$  dropped during morphogenesis of FPPase into CPPase and shifted from  $\text{CE}^{\text{DMAPP}}$   
47  
48  $< \text{CE}^{\text{GPP}} > \text{CE}^{\text{DMAPP}}$  to  $\text{CE}^{\text{DMAPP}} > \text{CE}^{\text{GPP}}$ , with a concomitant preference for synthesis of GPP. From  
49  
50 FPPase to C3,  $\text{CE}^{\text{DMAPP}}$  decreased 31-fold, while  $\text{CE}^{\text{GPP}}$  decreased 393-fold. From C3 to C10,  
51  
52  $\text{CE}^{\text{DMAPP}}$  was similar, while  $\text{CE}^{\text{GPP}}$  continued to decline (10<sup>3</sup>-fold, 10<sup>6</sup>-fold relative to  
53  
54  
55  
56  
57  
58  
59  
60

FPPase). Beginning at C11,  $CE^{DMAPP}$  dropped substantially, followed by smaller decreases to a  $CE^{DMAPP}$  for CPPase that was  $10^4$ -fold less than for FPPase. Values for  $CE^{GPP}$  cannot be measured for these enzymes because of a combination of low  $k_{cat}$ s and high  $K_M^{DMAPP}$ s. During morphogenesis of CPPase to FPPase, activity for chain elongation remained low, except for a spike at F10 from lower values for  $K_M^{DMAPP}$  and  $K_M^{GPP}$  (also observed at F1), for which we have no explanation.

**Table 3.** Kinetic constants for chain elongation.<sup>a</sup>

	$k_{cat}^{DMAPP}$ ( $s^{-1}$ )	$k_{cat}^{GPP}$ ( $s^{-1}$ )	$K_M^{DMAPP}$ ( $\mu M$ )	$K_M^{GPP}$ ( $\mu M$ )	$K_M^{IPP}$ ( $\mu M$ )
FPPase	$0.96 \pm 0.09$	$2.6 \pm 0.1$	$9 \pm 2$	$1.1 \pm 0.3$	$11 \pm 3$
C1	$1.2 \pm 0.1$	$1.5 \pm 0.1$	$4 \pm 1$	$3.5 \pm 0.9$	$12 \pm 5$
C2	$0.80 \pm 0.07$	$0.81 \pm 0.05$	$74 \pm 6$	$38 \pm 7$	$60 \pm 20$
C3	$0.63 \pm 0.06$	$0.22 \pm 0.01$	$200 \pm 20$	$36 \pm 7$	$23 \pm 7$
C4	$1.0 \pm 0.1$	$0.26 \pm 0.01$	$330 \pm 50$	$26 \pm 4$	$34 \pm 9$
C5	$0.61 \pm 0.04$	$0.23 \pm 0.01$	$110 \pm 20$	$16 \pm 3$	$14 \pm 3$
C6	$0.23 \pm 0.02$	$0.42 \pm 0.03$	$29 \pm 3$	$25 \pm 5$	$8 \pm 2$
C7	$0.188 \pm 0.008$	$0.147 \pm 0.009$	$140 \pm 20$	$240 \pm 50$	$11 \pm 2$
C8	$0.132 \pm 0.006$	$(7.7 \pm 0.3) \times 10^{-3}$	$18 \pm 2$	$680 \pm 70$	$14 \pm 2$
C10	$0.64 \pm 0.03$	$0.010 \pm 0.001$	$120 \pm 20$	$4000 \pm 800$	$59 \pm 10$
C11	$(7.0 \pm 0.6) \times 10^{-2}$	nd	$2000 \pm 300$	nd	$1300 \pm 400$
C12	$0.110 \pm 0.008$	nd	$2300 \pm 300$	nd	$1400 \pm 400$
C13	$(1.11 \pm 0.03) \times 10^{-2}$	nd	$350 \pm 50$	nd	$1600 \pm 400$
c-F-c	$(1.2 \pm 0.3) \times 10^{-2}$	nd	$290 \pm 50$	nd	$80 \pm 20$
CPPase	$(5.1 \pm 0.2) \times 10^{-3}$	nd	$510 \pm 90$	nd	$1700 \pm 200$
F1	$(1.25 \pm 0.09) \times 10^{-3}$	$(3.2 \pm 0.1) \times 10^{-4}$	$150 \pm 30$	$6.1 \pm 0.9$	$18 \pm 2$
F8	$(2.1 \pm 0.1) \times 10^{-3}$	$3.2 \times 10^{-3}$ (247 $\mu M$ ) <sup>b</sup>	$1000 \pm 300$	nd	$1000 \pm 200$
F9	$(9.1 \pm 0.4) \times 10^{-3}$	$8.9 \times 10^{-3}$ (247 $\mu M$ ) <sup>b</sup>	$1000 \pm 200$	nd	$2000 \pm 300$
F10	$(6.7 \pm 0.4) \times 10^{-3}$	$(7.1 \pm 0.4) \times 10^{-3}$	$14 \pm 4$	$7 \pm 2$	$11 \pm 2$
F11	$(2.7 \pm 0.1) \times 10^{-3}$	$1.7 \times 10^{-3}$ (247 $\mu M$ ) <sup>b</sup>	$1100 \pm 300$	nd	$1600 \pm 300$
F12	$(1.77 \pm 0.06) \times 10^{-3}$	$3.1 \times 10^{-3}$ (82 $\mu M$ ) <sup>b</sup>	$440 \pm 80$	nd	$1200 \pm 100$
F13	$(3.7 \pm 0.2) \times 10^{-3}$	$3.0 \times 10^{-3}$ (247 $\mu M$ ) <sup>b</sup>	$400 \pm 70$	nd	$2800 \pm 400$
f-C-f	$(8.7 \pm 0.3) \times 10^{-3}$	$9.7 \times 10^{-3}$ (247 $\mu M$ ) <sup>b</sup>	$530 \pm 70$	nd	$3300 \pm 300$

<sup>a</sup>[DMAPP] and [IPP] were optimized to give maximal values for  $k_{\text{cat}}$ . Apparent kinetic constants were determined at a fixed optimal [substrate 1] for varied [substrate 2]. nd- not determined. <sup>b</sup>Values for  $K_M^{\text{GPP}}$  were not determined because of low turnover, large differences in optimal concentrations of IPP and GPP and substrate inhibition at high [IPP].  $k_{\text{cat}}^{\text{GPP}}$  is an apparent value at optimal [GPP] and 6 mM IPP. Where no values for  $K_M^{\text{GPP}}$  are listed,  $k_{\text{cat}}$  is an apparent value at the indicated [GPP].

The catalytic efficiencies for synthesis of CPP and LPP from two molecules of DMAPP ( $k_{\text{cat}}^{\text{DMAPP}}/K_{50}^{\text{DMAPP}}$ ) and for synthesis of GPP from IPP and DMAPP ( $k_{\text{cat}}^{\text{DMAPP}}/K_M^{\text{DMAPP}}$ ) by CPPase were ~10,000-fold lower than for synthesis of GPP by FPPase (Tables 4 and 5). During morphogenesis of CPPase to FPPase, the rate for synthesis of the irregular products dropped 10-fold for the F1 chimera and 100- to 1000-fold for the remaining chimeras in the series. Irregular activity was not detected for FPPase. For the FPPase to CPPase series, a low level of irregular activity was first detected for C1 and remained low through C12, where  $k_{\text{cat}}^{\text{DMAPP}}$  was ~20-50-fold was lower than that for wt CPPase. For these chimeras, catalytic efficiencies for the irregular couplings were substantially less than for chain elongation and the major irregular products from branching (LPP) and cyclobutanation (MPP) were typically not detected in competition with chain elongation. At C13,  $k_{\text{cat}}^{\text{DMAPP}}$  increased to a level similar to CPPase. However, LPP was the major irregular product and the catalytic efficiency for chain elongation was ~6-fold greater than that for irregular coupling. In comparison, CPP was the dominant irregular product for CPPase, and the catalytic efficiencies for irregular coupling and chain elongation were similar.

**Table 4.** Catalytic efficiencies for chain elongation.

	$k_{\text{cat}}^{\text{DMAPP}}/K_{\text{M}}^{\text{DMAPP}}$ ( $\text{s}^{-1}\text{M}^{-1}$ )	$k_{\text{cat}}^{\text{GPP}}/K_{\text{M}}^{\text{GPP}}$ ( $\text{s}^{-1}\text{M}^{-1}$ )
FPPase	$1.0 \times 10^5$	$2.4 \times 10^6$
C1	$3.0 \times 10^5$	$4.3 \times 10^5$
C2	$1.1 \times 10^4$	$2.1 \times 10^4$
C3	$3.2 \times 10^3$	$6.1 \times 10^3$
C4	$3.0 \times 10^3$	$1.0 \times 10^4$
C5	$5.5 \times 10^3$	$1.4 \times 10^4$
C6	$7.9 \times 10^3$	$1.7 \times 10^4$
C7	$1.34 \times 10^3$	$6.1 \times 10^2$
C8	$7.3 \times 10^3$	11
C10	$5.3 \times 10^3$	2.5
C11	35	-
C12	48	-
C13	32	-
f-C-f	41	-
CPPase	10	-
F1	8.3	52
F8	2.1	-
F9	9.1	-
F10	$4.8 \times 10^2$	$1 \times 10^3$
F11	2.5	-
F12	4	-
F13	9.6	-
c-F-c	16	-

**Table 5.** Kinetic constants for formation of irregular products.

	$k_{\text{cat}}^{\text{DMAPP}}$ ( $\text{s}^{-1}$ )	$K_{50}^{\text{DMAPP}}$ ( $\mu\text{M}$ )	$k_{\text{cat}}/K_{50}^{\text{DMAPP}}$ ( $\text{s}^{-1} \text{M}^{-1}$ )
C1	$3.7 \times 10^{-4a}$	nd	-
C3	$6.9 \times 10^{-4a}$	nd	-
C4	$5.0 \times 10^{-4a}$	nd	-
C5	$1.1 \times 10^{-3a}$	nd	-
C6	$6.6 \times 10^{-4a}$	nd	-
C7	$9.5 \times 10^{-4a}$	nd	-
C8	$4.0 \times 10^{-4a}$	nd	-
C10	$9.6 \times 10^{-4a}$	nd	-
C11	$8.6 \times 10^{-4a}$	nd	-
C12	$5.9 \times 10^{-4a}$	nd	-
C13	$(1.1 \pm 0.05) \times 10^{-2}$	$2100 \pm 200$	5.2
f_C_f	$1.8 \times 10^{-3a}$	nd	-
CPPase	$(2.0 \pm 0.08) \times 10^{-2}$	$4100 \pm 400$	4.8
F1	$1.9 \times 10^{-3a}$	nd	-
F8	$3.2 \times 10^{-5a}$	nd	-
F9	$3.0 \times 10^{-4a}$	nd	-
F10	$6.3 \times 10^{-4a}$	nd	-

nd, not determined. <sup>a</sup>Measured at 6 mM DMAPP.

*Structural studies.* Models for *A. tridentata* FPPase·IPP·DMAPP, C13·IPP·DMAPP, C13·IPP·DMAPP, CPPase·IPP·DMAPP, and CPPase·DMAPP·DMAPP were constructed from X-ray structures of *E. coli* FPPase liganded with IPP and an unreactive thio analogue of DMAPP<sup>38, 39</sup> in a “closed” active conformation (Brookhaven PDB: 1RQI; 2.4 Å) and apo C13 (Brookhaven PDB: 4KK2; 2.2 Å). C13, which is the first chimera during the morphogenesis of FPPase to CPPase where formation of irregular products becomes competitive with chain elongation and the only protein in the *Artemisia* group whose crystal structure has

1  
2  
3 been reported, was used as the base structure for the modelling, as described in Supporting  
4  
5 Information.  
6

7  
8 Six active-site amino acids F92, A161, T194, F231, D235, and R343 in FPPase are  
9  
10 replaced by I92, I161, G194, Y231, N235, and G343, respectively, in CPPase. The locations  
11  
12 of substrates and amino acids at positions 193, 194, 231, 235 and 343 in the *A. tridentata*  
13  
14 enzymes are shown in Figure 6 with IPP in the acceptor region of *A. tridentata* FPPase (part  
15  
16 A) and IPP (part B) or DMAPP (part C) in the acceptor region of *A. tridentata* CPPase.  
17

18  
19 DMAPP is located in the donor regions of the active sites. In each case, the structures are  
20  
21 oriented so carbon-2 in the substrate in the acceptor site is located directly behind carbon-  
22  
23 3. This orientation highlights the differences among the conformations of the hydrocarbon  
24  
25 moieties of isopentenyl and dimethylallyl bound in the acceptor site. For IPP, the carbon  
26  
27 atoms attached to carbon-3 are restricted to a common plane and carbon-1 located above  
28  
29 the plane. In *A. tridentata* FPPase·IPP·DMAPP, the dihedral angle between carbon-1 and the  
30  
31 methyl group ( $\Theta$ ) is  $75^\circ$ , which is similar to the dihedral angle seen in *E. coli*  
32  
33 FPPase·IPP·DMAPP.<sup>29</sup> For *A. tridentata* CPPase·IPP·DMAPP,  $\Theta = 31^\circ$ . In contrast to IPP, all  
34  
35 of the carbon atoms in the dimethylallyl moiety are restricted to a common plane ( $\Theta = 0^\circ$ ).  
36  
37 Corresponding active site structures for C13 are essentially identical to those for CPPase.  
38  
39  
40  
41  
42

43  
44 In FPPase, F231 is located perpendicular to the plane of C2, C3, C4, and the methyl  
45  
46 group in IPP with its edge  $\sim 4 \text{ \AA}$  above the C3-C4 double bond in position to stabilize  
47  
48 developing positive charge in the IPP moiety during the electrophilic alkylation reaction.  
49  
50 One of the terminal R343 guanidinium nitrogens is located  $\sim 3.4 \text{ \AA}$  almost directly above  
51  
52 the center of the F231 aromatic ring. The other terminal nitrogen is located  $3.9 \text{ \AA}$  from one  
53  
54 of the non-bonding P1 oxygen atoms in IPP. R343 seems to have two roles – to help  
55  
56  
57  
58  
59  
60

1  
2  
3 immobilize the diphosphate group in IPP and to lock the aromatic ring of F231 over the  
4 double bond in IPP. D235 is part of the DDXXD motif that binds the diphosphate unit in  
5  
6 DMAPP. The carboxylate group in D235 is coordinated with one of the active site  
7  
8 magnesium atoms that bind DMAPP diphosphate and the two carboxylate oxygens are  
9  
10 about  $\sim 3.5$  Å from the IPP methyl group. The side chain hydroxyl group in T194 is  
11  
12 hydrogen bonded to the amide carbonyl of G228 and the T194 methyl group is 4.8 Å from  
13  
14 the methylene carbon at C4 in IPP. The amino group in K193 helps bind the DMAPP  
15  
16 diphosphate groups in FPPase·IPP·DMAPP and CPPase·IPP·DMAPP. The non-conserved  
17  
18 amino acids at positions 92 and 161 in FPPase and CPPase are located in a hydrophobic  
19  
20 pocket that interacts with the terminal isoprene unit in GPP and do not make contact with  
21  
22 DMAPP.  
23  
24  
25  
26  
27  
28  
29

30 In CPPase, the plane of the aromatic ring in Y231 makes a  $\sim 50^\circ$  angle with the plane  
31  
32 of the C1-C4 carbons in IPP and its edge is 3.6 Å above the IPP methyl group. The  
33  
34 diphosphate moiety in IPP is anchored to Y231 by a hydrogen bond between a non-  
35  
36 bonding P1 oxygen and the hydroxyl group in the tyrosine side chain. The amide group in  
37  
38 N235 is twisted relative to the position of the D235 carboxylate in FPPase and is located 3.1  
39  
40 Å from the IPP methyl group. The backbone chain of G194 is displaced toward IPP in  
41  
42 CPPase relative to the T194 backbone, and is located 4.8 Å from the IPP C4 methylene  
43  
44 carbon. Water molecules occupy similar locations in the active sites of FPPase and CPPase  
45  
46 where they coordinate with the three magnesium atoms that bind to the diphosphate in  
47  
48 DMAPP and form a shell around the diphosphate in IPP.  
49  
50  
51  
52  
53  
54  
55  
56  
57  
58  
59  
60

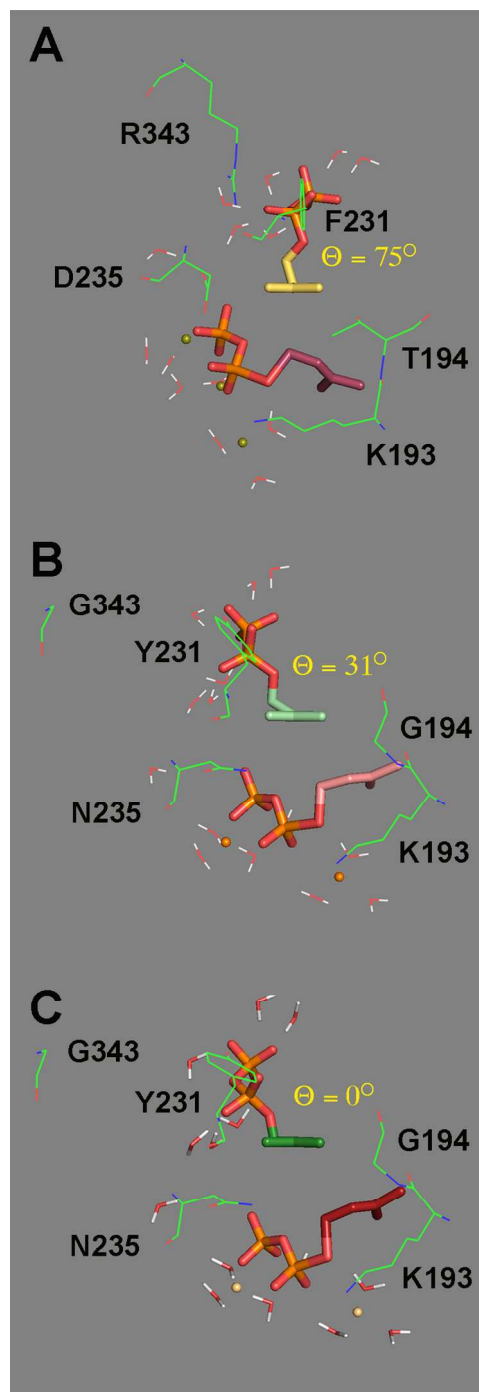


**Figure 6.** Active site structures for *A. tridentata* FPPase and CPPase. Part A: FPPase·IPP·DMAPP - isopentenyl moiety (yellow), dimethylallyl moiety (raspberry), Mg<sup>2+</sup> (olive); Part B: CPPase·IPP·DMAPP - isopentenyl moiety (pale green), dimethylallyl moiety (salmon), Mg<sup>2+</sup> (orange); Part C: CPPase·DMAPP·DMAPP - dimethylallyl moiety (isopentenyl region, forest green), dimethylallyl moiety (firebrick red), Mg<sup>2+</sup> (light orange).

1  
2  
3  
4  
5  
6  
7  
8  
9  
10  
11  
12  
13  
14  
15  
16  
17  
18  
19  
20  
21  
22  
23  
24  
25  
26  
27  
28  
29  
30  
31  
32  
33  
34  
35  
36  
37  
38  
39  
40  
41  
42  
43  
44  
45  
46  
47  
48  
49  
50  
51  
52  
53  
54  
55  
56  
57  
58  
59  
60

Figure 7 (part A) shows active site overlays for *A. tridentata* FPPase·IPP·DMAPP and *A. tridentata* CPPase·IPP·DMAPP and are arranged to superimpose the carbon-2-carbon-3 bonds of the substrates in the acceptor sites. The only substantial conformational changes seen between the active site amino acids in FPPase and CPPase relative to the substrates are at positions 194, 231, and 235. The side chains in F231 and Y231 are positioned to stabilize the tertiary carbocationic intermediate formed during the alkylation step (see Scheme 1). However, the Y231 aromatic ring in CPPase is displaced upward toward phosphorus-1 in IPP relative to the F231 phenyl group in FPPase. The IPP methyl group is located above the D235 carboxylate equidistant from both carboxylate oxygens. In contrast, the amide group in N235 side chain amide of CPPase is displaced upward to within hydrogen bonding distance of the bond-bridging oxygens of P2 in DMAPP. These changes alter the topology of the binding pocket occupied for the methyl group in IPP and move C1 in IPP toward the plane of the four other carbon atoms in IPP. The T194 to G194 mutation allows the binding pocket to accommodate methylene group as the dihedral angle in IPP decreases from 75° in FPPase to 31° in CPPase. As shown in Figure 7 (part B), CPPase can accommodate either IPP or DMAPP in the acceptor region of the active site by small changes in the conformation of the diphosphate moiety and the tilt of the aromatic ring in Y231.

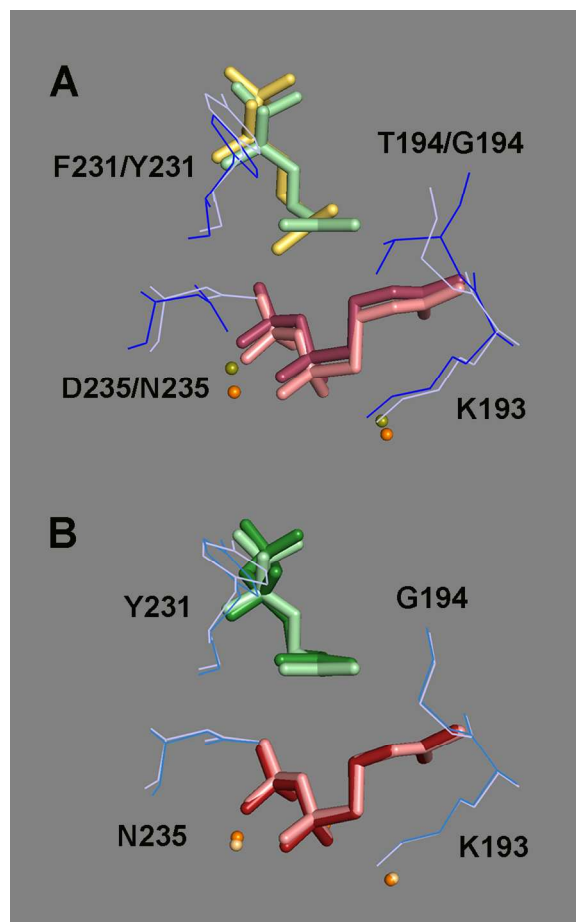


**Figure 7.** Overlays of active sites of *A. tridentata* FPPase and CPPase. Part A: FPPase·IPP·DMAPP – IPP (yellow), DMAPP (raspberry), Mg<sup>2+</sup> (olive), and amino acids (blue); CPPase·IPP·DMAPP – IPP (pale green), DMAPP (salmon), Mg<sup>2+</sup> (orange), and amino acids (sky blue). Part B: CPPase·IPP·DMAPP – IPP (pale green), DMAPP (salmon), Mg<sup>2+</sup> (orange), and amino acids (sky blue); CPPase·DMAPP·DMAPP – DMAPP (acceptor, dark green; donor, firebrick red), Mg<sup>2+</sup> (light orange), and amino acids (light blue).

## DISCUSSION

The  $\alpha$  terpenoid synthase fold, found in all members of CL0613, most likely evolved from a gene duplication-fusion event of a primordial 4-helix bundle protein.<sup>10</sup> Presumably an ancestral fusion protein, with hallmark DDXXD/DDXXD motifs on mirror image helices, evolved the ability to bind an allylic diphosphate and catalyze the electrophilic alkylation

1  
2  
3 reactions required for chain elongation to synthesize the linear isoprenoid diphosphates  
4 (PF00348), which lie at the core of the isoprenoid biosynthetic pathway. Subsequent  
5  
6 mutations provide a logical pathway for evolution of cyclopropanation/rearrangement  
7  
8 enzymes with DTLED/DYKED motifs (PF00494), and cyclases with  
9  
10 DDXXD/(N,D)D(L,I,V)X(S,T)XXXE motifs (PF03936, PF01397) located at similar positions  
11  
12 in the  $\alpha$ -terpenoid synthase fold. Chain elongation is an essential activity, and enzymes  
13  
14 belonging to PF00348 are found all forms of life. The cyclopropanation-rearrangement  
15  
16 enzymes in PF00494 are not universally distributed, but they are required for biosynthesis  
17  
18 of sterols,<sup>23</sup> carotenoids,<sup>18</sup> and membrane-affiliated pentacyclic triterpenes<sup>40</sup> in Archaea,  
19  
20 Bacteria, and Eukaryota.  
21  
22  
23  
24  
25  
26

27  
28 Carbocations are remarkably indiscriminate in their cyclizations, rearrangements,  
29  
30 and reactions with nucleophiles. As a group, the  $\alpha$  terpenoid synthases, which catalyze  
31  
32 electrophilic reactions through carbocationic intermediates, are highly promiscuous.<sup>10</sup>  
33  
34 Many of the wild-type enzymes give multiple products and seemingly minor mutations in  
35  
36 highly selective  $\alpha$  terpenoid synthases often result in promiscuous behavior. This behavior  
37  
38 has apparently been exploited during evolution of the isoprenoid pathway to produce the  
39  
40 unusually large number of different carbon skeletons found among isoprenoid  
41  
42 compounds.<sup>1</sup>  
43  
44  
45

46  
47 *A. tridentata* CPPase is an example where a parental FPPase, which is highly  
48  
49 optimized to synthesize FPP from IPP and DMAPP, has evolved the capability to synthesize  
50  
51 CPP, LPP, and much less efficiently, MPP from DMAPP. In contrast to some highly selective  
52  
53 terpenoid cyclases, where a single mutation can introduce significant promiscuous  
54  
55 behavior,<sup>10</sup> the architecture of FPP synthase robustly supports chain elongation. Although  
56  
57  
58  
59  
60

1  
2  
3 trace amounts of irregular products were seen early during morphogenesis of FPPase to  
4  
5 CPPase when DMAPP is the sole substrate, they were not detected in incubations with IPP  
6  
7 and DMAPP, where chain elongation is a competitive reaction, until the process had  
8  
9 reached the C13 chimera and all of the FPP helices surrounding the active site were  
10  
11 replaced by the corresponding helices from CPP. Likewise, no irregular products were  
12  
13 formed in competition with chain elongation in the site-directed mutants. In contrast,  
14  
15 formation of irregular products in competition with chain elongation ceased very early  
16  
17 during morphogenesis of CPPase to FPPase.  
18  
19  
20  
21

22 Evolution of FPPase to CPPase involves changes in substrate binding to favor  
23  
24 DMAPP over GPP in the donor site and permit DMAPP to compete with IPP for the acceptor  
25  
26 site. The selectivity of the donor site in FPPase can be altered to favor binding DMAPP over  
27  
28 GPP in a straightforward manner by reducing the size of the hydrophobic pocket.<sup>41</sup> In  
29  
30 contrast, the ability to exclude DMAPP from the acceptor site is a highly conserved feature  
31  
32 of chain elongation enzymes that is difficult to manipulate. A major factor that allows  
33  
34 FPPase to discriminate between IPP and DMAPP appears to be related to differences in the  
35  
36 conformational flexibility of the two molecules.<sup>42</sup> The hydrocarbon moiety in DMAPP is  
37  
38 rigid, with all of its carbon atoms confined to a common plane, while rotation about the  
39  
40 carbon-1-carbon-2 bond in IPP allows carbon-1 to move out of the plane. In the *A.*  
41  
42 *tridentata* FPPase·IPP·DMAPP ternary complex, carbon-1 is displaced from the plane by  
43  
44 ~75° to give a conformation that cannot be duplicated by DMAPP. In contrast, the out of  
45  
46 plane displacement for carbon-1 of IPP in *A. tridentata* CPPase·IPP·DMAPP complex is only  
47  
48 31°, and the bound conformations of IPP and DMAPP in the acceptor site of *A. tridentata*  
49  
50  
51  
52  
53  
54  
55  
56  
57  
58  
59  
60 CPPase are similar (Figure 7B).

1  
2  
3 Six active site amino acids in FPPase, F92, A161, T194, F231, D235, and R343, are  
4 not conserved in CPPase. Site-directed FPPase mutants where one or more of these  
5 residues are replaced with the corresponding amino acids from CPPase catalyze chain  
6 elongation with no detectable amounts of irregular products in incubations with IPP and  
7 DMAPP, including the 6m mutant, where all six of the amino acids are replaced. Trace  
8 quantities of LPP and MPP are seen when 6m-FPPase is incubated with DMAPP, similar to  
9 the behavior observed in the C1-C12 chimeras.  
10  
11  
12  
13  
14  
15  
16  
17  
18  
19

20 Kinetic constants for FPPase, CPPase, and the mutant proteins reflect these  
21 differences in substrate binding at the donor and acceptor sites. For chain elongation,  $K_M^{GPP}$   
22 increases >4000-fold during the morphogenesis of FPPase to CPPase, while  $K_M^{DMAPP}$   
23 increases only ~50 fold. A concomitant ~170-fold increase in  $K_M^{IPP}$  results in a 10,000-fold  
24 decrease in catalytic efficiency ( $k^{cat} / K_M$ ) for the chain elongation reaction. FPPase does not  
25 synthesize irregular products from DMAPP, even under forcing conditions. Very low levels  
26 of branching and cyclobutanation products are seen for incubations of the C1-C12 chimeras  
27 but are only be detected when DMAPP is the sole substrate. At C13, where all of the  $\alpha$   
28 terpenoid synthase fold in FPPase is replaced, the activity for synthesis of irregular  
29 products increases substantially and competes with chain elongation in incubations with  
30 IPP and DMAPP, with CPP and LPP constituting 11% of the products. The final  
31 morphogenesis of C13 to wild type *A. tridentata* CPPase results in small adjustments that  
32 increase the ratio of irregular to chain elongation products from ~1:10 to ~1:1 and the  
33 ratio of irregular products CPP to LPP from ~1:3 to 3:1.  
34  
35  
36  
37  
38  
39  
40  
41  
42  
43  
44  
45  
46  
47  
48  
49  
50  
51  
52

53 The amino acids at positions 194, located at the VIIa/VIIb kink in helix VII, and at  
54 positions 231 and 235 in helix VIII are in contact with the hydrocarbon moiety IPP in  
55  
56  
57  
58  
59  
60

1  
2  
3 FPPase·IPP·DMAPP and CPPase·IPP·DMAPP. In FPPase, the IPP methyl group and the C4  
4 methylene carbon are approximately equidistant ( $\sim 4 \text{ \AA}$ ) from the edge of the aromatic ring  
5 of F231 and the methyl group is  $\sim 3.5 \text{ \AA}$  above the plane of the D235 carboxylate (Figure  
6 8A). Rotations away from the  $75^\circ$  angle will generate unfavorable steric interactions with  
7 the edge of the aromatic ring. The positions of Y231 aromatic ring the N235 amide groups  
8 in CPPase·IPP·DMAPP are both “tilted” relative to their conformations in  
9 FPPase·IPP·DMAPP to reduce the twist in IPP to  $31^\circ$  (Figure 8B). A shift in the location of  
10 helix VIII in CPPase·IPP·DMAPP with respect to the rest of the six-helix bundle moves the  
11 binding pocket for the methyl group in IPP, defined by amino acids at positions 231 and  
12 235, “upward” relative to their locations in FPPase. This motion relaxes the sterically  
13 induced twist about the C2-C3 bond in IPP from  $\Theta$  from  $75^\circ$  in FPPase·IPP·DMAPP to  $31^\circ$  in  
14 13C·IPP·DMAPP (Figure 8C). The accompanying “downward” motion of the olefinic  
15 methylene group in IPP is accommodated by the space created by the mutation T194G.  
16  
17

18  
19  
20  
21  
22  
23  
24  
25  
26  
27  
28  
29  
30  
31  
32  
33  
34  
35 In FPPase·IPP·DMAPP the distances between C1 of DMAPP and the C3-C4 olefinic  
36 carbons in IPP are 3.3 and  $3.6 \text{ \AA}$ , respectively, and increase to 3.9 and  $4.0 \text{ \AA}$  in  
37 CPPase·IPP·DMAPP. In CPPase·DMAPP·DMAPP, the distances between C1 of the donor  
38 DMAPP and the C2-C3 olefinic carbons in the acceptor DMAPP are 4.1 and  $4.2 \text{ \AA}$ . These  
39 distances between electrophile and nucleophile in the FPPase and CPPase complexes are  
40 compatible with a dissociative electrophilic alkylation by the double bonds in IPP and  
41 DMAPP by the electrophilic dimethylallyl cation sandwiched between the acceptor  
42 substrate and the inorganic pyrophosphate leaving group.  
43  
44  
45  
46  
47  
48  
49  
50  
51  
52

53  
54 The conformations for FPPase·IPP·DMAPP, CPPase·IPP·DMAPP, and  
55 CPPase·DMAPP·DMAPP shown in Figure 8 indicate how the active site is remolded to  
56  
57  
58  
59  
60

1  
2  
3 accommodate DMAPP in the acceptor region. However, the minimum number of mutations  
4  
5 needed to convert FPPase to a catalyst where CPP is a major product is not obvious. While  
6  
7 substitutions of some active site residues are required for the remodeling, it is apparent that  
8  
9 amino acid substitutions outside of the active site are important. This is illustrated by  
10  
11 replacing the scaffold around the six-helix bundle core of CPPase with the scaffold from  
12  
13 FPPase, resulting in a ~2-fold increase in LPP and a 35-fold decrease in CPP. The ability of  
14  
15 seemingly small changes in the active sites of FPPase and CPPase, and even less apparent  
16  
17 changes distal to the active site, to alter the course of the reactions they catalyze is a  
18  
19 characteristic of many enzymes in the terpenoid synthase superfamily, especially those in  
20  
21 the cyclase groups PF01397 and PF03936,<sup>10</sup> and is a consequence of the sensitivity of  
22  
23 carbocations to their environments.  
24  
25  
26  
27  
28  
29  
30  
31  
32  
33  
34  
35  
36  
37  
38  
39  
40  
41  
42  
43  
44  
45  
46  
47  
48  
49  
50  
51  
52  
53  
54  
55  
56  
57  
58  
59  
60

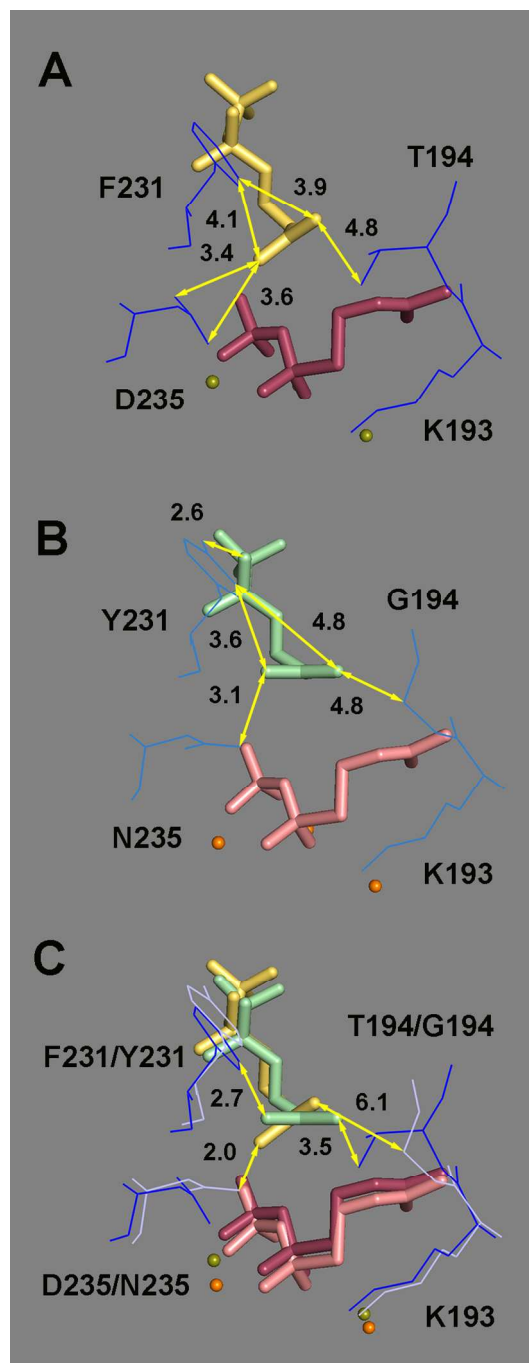


**Figure 8.** Interactions between C4 olefinic methylene group and the methyl group in IPP with amino acids at positions 231 and 235 in *A. tridentata* FPPase and CPPase. Same color-coding as Figure 6. Part A: FPPase. Part B: CPPase. Part C: an overlay of FPPase and CPPase.

## CONCLUSIONS

*A. tridentata* FPPase and CPPase are closely related proteins. FPPase catalyzes the chain elongation of DMAPP to FPP by sequential addition of two molecules of IPP, while CPPase catalyzes chain elongation of DMAPP to GPP along with condensation of two molecules of DMAPP to give irregular isoprenoid carbon skeletons with cyclopropane, branched, and cyclobutane structures. Stepwise replacement of the helices and loops surrounding the active site of FPPase by the corresponding regions from CPPase results in the gradual metamorphosis of the selective efficient chain elongation enzyme to a promiscuous relative that inefficiently catalyzes chain elongation and cyclopropanation/branching/cyclobutanation reactions. The initial replacements shift the preference for synthesis of FPP to GPP, accompanied by a moderate loss in catalytic efficiency. Formation of irregular products only become competitive with chain elongation upon replacement of helix VIII. Structural models suggest that the high selectivity for chain elongation by FPPase results because IPP binds to the acceptor region of the active site in a conformation that cannot be adopted by DMAPP. Synthesis of irregular products becomes competitive with chain elongation when the topology of the active site allows IPP and DMAPP to be bound in similar conformations.

*A. tridentata* CPPase is an example of an enzyme that has evolved recently from a highly-specialized parent. The origins of FPPase date back to the very beginning of cellular life, and the enzyme has perfected its ability to catalyze chain-elongation. In contrast, *A. tridentata* CPPase has recently evolved from *A. tridentata* FPPase, presumably by gene duplication and random mutagenesis<sup>43</sup> but is still a promiscuous inefficient catalyst in comparison with FPPase. While the biosynthesis of irregular monoterpenes provides no

1  
2  
3 obvious benefit to sagebrush, the insecticidal properties of pyrethrum synthesized from  
4  
5 CPP by *C. cinerifolium* could provide continual evolutionary pressure for optimization of  
6  
7 CPPase.<sup>22</sup> The approximately 80,000 occurring isoprenoid compounds found in nature,  
8  
9 with numerous different carbon skeletons often formed from the same substrates, is a  
10  
11 testament to the ability of enzyme evolution to harness the inherent diversity of  
12  
13 carbocation chemistry.  
14  
15  
16  
17  
18  
19

## 20 ASSOCIATED CONTENT

### 21 Supporting Information

22  
23 Experimental section; strategy for construction of expression vectors for FPPase:CPPase  
24  
25 chimeras (Figure S1); representative GC-FID traces of enzymatic products (Figures S2 –  
26  
27 S3); EI/MS spectra of hydrolyzed enzymatic products (Figures S4 – S11); DNA sequences of  
28  
29 CPPase and FPPase synthesized in *E. coli* context (Figures S12 – S13); representative  
30  
31 hyperbolic plots for the determination of apparent Michaelis-Menten kinetic parameters  
32  
33 (Figures S14– S17); representative TLC, UPLC-MS, GC, and MS analyses of enzymatic  
34  
35 products (Figures S18 – S22); PCR crossover primers used in the production of the  
36  
37 chimeric genes (Table S1); representative ESI/MS of enzymes for molecular weight  
38  
39 verification (Table S2). This material is available free of charge at <http://pubs.acs.org>.  
40  
41  
42  
43  
44  
45  
46  
47  
48

## 49 AUTHOR INFORMATION

### 50 Corresponding author

51  
52 [poulter@chemistry.utah.edu](mailto:poulter@chemistry.utah.edu)  
53  
54  
55  
56  
57  
58  
59  
60

1  
2  
3 **Present address**  
4

5  
6 †**Mucosal Inflammation Program, Department of Medicine, University of Colorado**  
7

8  
9 **Anschutz Medical Campus, Aurora, Colorado 80045**  
10

11 **Notes**  
12

13  
14 The authors declare no competing financial interest.  
15

16 **ACKNOWLEDGEMENTS**  
17

18  
19 This work was supported by a grant from the National Institute of General Medical  
20  
21 Sciences (GM 21328).  
22

23 **REFERENCES**  
24

- 25  
26 1. Buckingham, J.; Cooper, C.M.; Purchase, R. *Natural Products Reference Desk* **2016**, Boca  
27 Raton: CRC Press, Taylor & Francis Group, p. 235.  
28  
29 2. Thulasiram, H. V.; Erickson, H. K.; Poulter, C. D. *J. Am. Chem. Soc.* **2008**, *130*, 1966-1971.  
30  
31 3. Tarshis, L. C.; Proteau, P. J.; Kellogg, B. A.; Sacchettini, J. C.; Poulter, C. D. *Proc. Natl. Acad.*  
32 *Sci. USA* **1996**, *93*, 15018-15023.  
33  
34 4. Poulter, C. D., *Phytochem. Rev.* **2006**, *5* (1), 17-26.  
35  
36 5. Christianson, D. W. *Current Opinion in Chemical Biology* **2008**, *12*, 141-150.  
37  
38 6. Thulasiram, H. V.; Erickson, H. K.; Poulter, C. D. *Science* **2007**, *316*, 73.  
39  
40 7. EBML-EBI [http://pfam.xfam.org/family/polyprenyl\\_synt#tabview=tab2](http://pfam.xfam.org/family/polyprenyl_synt#tabview=tab2)  
41  
42 8. Tarshis, L. C.; Yan, M.; Poulter, C. D.; Sacchettini, J. C. *Biochemistry* **1994**, *33*, 10871-  
43 10877.  
44  
45 9. Cao, R.; Zhang, Y.; Mann, F. M.; Huang, C.; Mukkamala, D.; Hudock, M. P.; Mead, M. E.;  
46 Pristic, S.; Wang, K.; Lin, F.-Y.; Chang, T.-K.; Peters, R. J.; Oldfield, E. *Struct., Funct., Bioinf.*  
47 **2010**, *78*, 2417-2432.  
48  
49 10. Christianson, D.W. *Chem. Rev.* **2017**, *117*, 11570-11648.  
50  
51 11. Fujihashi, M.; Zhang, Y.-W.; Higuchi, Y.; Li, X.-Y.; Koyama, T.; Miki, K. *Proc. Natl. Acad. Sci.*  
52 *USA* **2001**, *98*, 4337-4342.  
53  
54  
55  
56  
57  
58  
59  
60

- 1  
2  
3  
4  
5 12. Paterson-Jones, J. C.; Gilliland, M. G.; Van Staden, J. *J. Plant Physio.* **1990**, *136*, 257-263.  
6  
7 13. Poulter, C. D.; Rilling, H. C. *Acc. Chem. Res.* **1978**, *11*, 307-313.  
8  
9 14. Thulasiram, H. V.; Poulter, C. D. *J. Am. Chem. Soc.* **2006**, *128*, 15819-15823  
10  
11  
12 15. Resh, M. D. *Nat. Chem. Biol.* **2006**, *2*, 584-590.  
13  
14 16. Poulter, C. D.; Marsh, L. L.; Hughes, J. M.; Argyle, J. C.; Satterwhite, D. M.; Goodfellow,  
15 R. J.; Moesinger, S. G. *J. Am. Chem. Soc.* **1977**, *99*, 3816-3823.  
16  
17 17. Rilling, H. C.; Epstein, W. W. *J. Am. Chem. Soc.* **1969**, *91*, 1041-1042.  
18  
19 18. Altman, L. J.; Ash, L.; Kowerski, R. C.; Epstein, W. W.; Larsen, B. R.; Rilling, H. C.; Muscio,  
20 F.; Gregonis, D. E. *J. Am. Chem. Soc.* **1972**, *94*, 3257-3259.  
21  
22 19. Gunawardena, K.; Rivera, S. B.; Epstein, W. W. *Phytochem.* **2002**, *59*, 197-203.  
23  
24 20. Zhang, A.; Amalin, D.; Shirali, S.; Serrano, M. S.; Franqui, R. A.; Oliver, J. E.; Klun, J. A.;  
25 Aldrich, J. R.; Meyerdirk, D. E.; Lapointe, S. L. *Proc. Natl. Acad. Sci. USA* **2004**, *101*, 9601-  
26 9606.  
27  
28 21. Bierl-Leonhardt, B. A.; Moreno, D. S.; Schwarz, M.; Fargerlund, J.; Plimmer, J. R. *Tet. Lett.*  
29 **1981**, *22*, 389-392.  
30  
31 22. Rivera, S. B.; Swedlund, B. D.; King, G. J.; Bell, R. N.; Hussey, C. E.; Shattuck-Eidens, D. M.;  
32 Wrobel, W. M.; Peiser, G. D.; Poulter, C. D. *Proc. Natl. Acad. Sci.* **2001**, *98*, 4373-4378.  
33  
34 23. Epstein, W. W.; Rilling, H. C. *J. Biol. Chem.* **1970**, *245*, 4597-4605.  
35  
36 24. Pandit, J.; Danley, D. E.; Schulte, G. K.; Mazzalupo, S.; Pauly, T. A.; Hayward, C. M.;  
37 Hamanaka, E. S.; Thompson, J. F.; Harwood, H. J. *J. Biol. Chem.* **2000**, *275*, 30610-30617.  
38  
39 25. Pan, J.J.; Solbiati, J.O.; Ramamoorthy, G.; Hillerich, B.S.; Seidel, R.D. Cronan, J.E.; Almo,  
40 S.C.; Poulter, C.D. *ACS Cent. Sci.* **2015**, 77-82.  
41  
42 26. Iwata-Reuyl, D.; Math, S. K.; Desai, S. B.; Poulter, C. D. *Biochemistry* **2003**, *42*, 3359-3365  
43  
44 27. Demissie, Z. A.; Erland, L. A. E.; Rheault, M. R.; Mahmoud, S. S. *J. Biol. Chem.* **2013**, *288*,  
45 6333-6341.  
46  
47 28. Chayet, L.; Rojas, M. C.; Cori, O.; Bunton, C. A.; McKenzie, D. C. *Bioorg. Chem.* **1984**, *12*,  
48 329-338.  
49  
50  
51  
52  
53  
54  
55  
56  
57  
58  
59  
60

- 1  
2  
3  
4  
5  
6  
7  
8  
9  
10  
11  
12  
13  
14  
15  
16  
17  
18  
19  
20  
21  
22  
23  
24  
25  
26  
27  
28  
29  
30  
31  
32  
33  
34  
35  
36  
37  
38  
39  
40  
41  
42  
43  
44  
45  
46  
47  
48  
49  
50  
51  
52  
53  
54  
55  
56  
57  
58  
59  
60
29. Hosfield, D. J.; Zhang, Y.; Dougan, D. R.; Broun, A.; Tari, L. W.; Swanson, R. V.; Finn, J. *J. Biol. Chem.* **2004**, *279*, 8526-8529.
30. Hemmerlin, A.; Rivera, S. B.; Erickson, H. K.; Poulter, C. D. *J. Biol. Chem.* **2003**, *278*, 32132-32140.
31. Bergthorsson, U.; Andersson, D. I.; Roth, J. R. *Proc. Natl. Acad. Sci. USA* **2007**, *104* (43), 17004-17009.
32. Chen, A.; Kroon, P. A.; Poulter, C. D. *Prot. Sci.* **1994**, *3*, 600-607.
33. Miyazaki, K.; Takenouchi, M. *Biotechniques* **2002**, *33*, 1033-4, 1036-8.
34. O'Maille, P. E.; Bakhtina, M.; Tsai, M.-D. *J. Mol. Biol.* **2002**, *321*, 677-691.
35. Laskovics, F. M.; Poulter, C. D. *Biochemistry* **1981**, *20*, 1893-1901.
36. Chen, M.; Poulter, C. D. *Biochemistry* **2010**, *49*, 207-217.
37. Laskovics, F. M.; Krafcik, J. M.; Poulter, C. D. *J. Biol. Chem.* **1979**, *254*, 9458-9463.
38. Phan, R. M.; Poulter, C. D. *J. Org. Chem.* **2001**, *66*, 6705-6710.
39. Phan, R. M.; Poulter, C. D. *Org. Lett.* **2000**, *2*, 2287-2289.
40. Prades, J.; Vögler, O.; Alemany, R.; Gomez-Florit, M.; Funari, S. S.; Ruiz-Gutiérrez, V.; Barceló, F. *Biochim. Biophys. Acta* **2011**, *1808*, 752-760.
41. Stanley Fernandez, S. M.; Kellogg, B. A.; Poulter, C. D. *Biochemistry* **2000**, *39*, 15316-15321.
42. Rilling, H. *Pure Appl. Chem.* **1979**, *51*, 597-608.
43. Näsvall, J.; Sun, L.; Roth, J. R.; Andersson, D. I. *Science* **2012**, *338*, 384.

